Plasmachemical Amine Functionalization of Porous Polystyrene Spheres: The Importance of Particle Size

G. Øye, V. Roucoules, L. J. Oates, A. M. Cameron, N. R. Cameron, P. G. Steel, and J. P. S. Badyal*

Department of Chemistry, Science Laboratories, Durham University, Durham DH1 3LE, England, U.K.

B. G. Davis

Dyson Perrins Laboratory, Department of Chemistry, University of Oxford, Oxford OX1 3QY, England, U.K.

D. M. Coe and R. A. Cox

GlaxoSmithKline, Medicines Research Centre, Gunnels Wood Road, Stevenage SG1 2NY, England, U.K.

Received: May 21, 2002; In Final Form: January 31, 2003

Allylamine plasma functionalization of porous polystyrene spheres is found to depend on particle size. A combination of Fmoc derivatization and cross-sectional Raman microscopy has shown that an outer layer of approximately 3−4 μm can be selectively functionalized to yield relatively high amine group loadings.

Introduction

Functionalized porous polymer beads are widely employed for solid-phase organic synthesis,[1,2] combinatorial chemistry,[3] polymer-supported catalysis,[4,5] and ion-exchange resins.[6,7] Typically, the functionality is incorporated into the porous polymer structure by copolymerization of monomers.[8] However, the number of commercial monomers is limited, which in turn restricts the available surface chemistry. An alternative approach is grafting techniques;[9] however, in this case a common drawback is side reactions leading to a detrimental impact on support performance.

In this article we describe the plasmachemical functionalization of porous polymer spheres. This approach can be regarded as being comparatively quick, cheap, and solventless.[10] In fact, there have already been a number of studies reported related to plasma modification of a variety of powders (to give oxygenated[11] siloxane,[12] fluorocarbon,[13,14] and amine[15,16] groups). However, there currently exists very little understanding concerning how the overall level of chemical modification is influenced by the physical properties of the porous particle (e.g., surface area, particle size, pore size distribution, etc.). The current investigation examines how the level of plasmachemical amine functionalization is governed by particle size (for a series of polystyrene beads all possessing similar pore architecture). Allylamine (CH_2═$CH-CH_2-NH_2$) has been employed as the precursor molecule for plasma polymerization, since it contains a polymerizable carbon−carbon double bond which is amenable to electrical discharge activation, while the primary amine group is a suitable candidate for application in solid-phase organic synthesis. A combination of BET surface area measurement, Fmoc derivatization of amine groups, and Raman microscopy have been employed to determine the level and spatial distribution of plasmachemical functionalization.

* Author to whom correspondence should be addressed.

Experimental Section

Porous polymer spheres were prepared by suspension polymerization.[17] This entailed dissolving stabilizers (2 g of poly(vinyl alcohol) and 2 g of sodium chloride) in 400 mL of hot water. Upon cooling, the solution was transferred into a 500 mL suspension polymerization reactor, followed by the addition of a mixture of monomer (5 mL of styrene), cross-linker (45 mL of divinylbenzene), porogen (50 mL of heptane), and initiator (0.5 g of azobisisobutyronitrile) at 32 °C, and then stirred at a speed of 1200 rpm. Next, the reactor was flushed with nitrogen gas for 10 min and the temperature of the surrounding water bath was raised to 80 °C for a period of 6 h. This produced polymer particles, which were separated by suction filtration from the hot solution. These were washed with hot distilled water, transferred to a Soxhlet thimble, extracted with water and acetone, and finally dried under vacuum at 50 °C. A particle size distribution ranging between 20 μm and 300 μm was obtained. This material was separated using 6 Endecotts' test sieves and an orbital shaker (Vibrax VXR) to give the following batches: D (20−38), D (38−53), D (53−90), D (90−125), D (125−180), and D (180−300), where the numbers in the brackets specify the particle size range in μm.

Nitrogen sorption measurements of the synthesized polystyrene beads were performed at 77 K (Micromeritics—TriStar 3000 Surface Area and Porosimetry Analyzer). Each sample was degassed at 50 °C for 12 h. The specific surface area and the pore volume were estimated according to the BET and BJH models, respectively.[18−20]

To ascertain how the level of plasmachemical functionalization is governed by particle size, two experimental approaches were adopted: Approach A, in which the polymer beads were sieved into different particle size ranges, and 250 mg of each type were individually plasma treated; Approach B, in which equal amounts of mass from each size range were mixed together to give a well-defined recombined sample composition, and then 250 mg of this material was plasma-modified.

10.1021/jp021262l CCC: $25.00
Published on Web 03/22/2003

Plasma polymerization experiments were carried out in a rotating plasma reactor pumped by a two-stage rotary pump (Edwards E2M2 Fomblin) via a liquid nitrogen cold trap (base pressure better than 2×10^{-2} mbar and a leak rate less than 1×10^{-3} mbar/min). A 13.56 MHz RF field (ACG-3 ENI generator) was applied via a matching network connected to a copper coil wound around the glass chamber. Prior to each plasma treatment, the reactor was cleaned with detergent, washed with water and propan-2-ol, followed by drying. Further cleaning entailed air plasma treatment at 0.2 mbar pressure and 50 W power for 30 min. At this stage, 250 mg of polymer bead material was loaded into the chamber and evacuated. Next, allylamine monomer vapor was introduced into the system at 0.4 mbar, and the electrical discharge ignited at 20 W power for 20 min. These parameters were optimized on the basis of a 2^{5-2} reduced factorial experimental design (power, pressure, time, rotation speed, and quantity), followed by Simplex optimization.

Quantification of the number of accessible amine groups present on the plasma-functionalized polystyrene beads comprised measuring the Fmoc loading.[21] This entailed washing the treated beads in methanol (2×1 mL), and then dichloromethane (2×1 mL) in order to remove any loosely bound material. Subsequent washing in a 20% piperidine/*N*,*N*-dimethylformamide solution (2×1 mL) dislodged any carbon dioxide adsorbed onto the amine groups. Next, the samples were dried under nitrogen gas, and 20 mg of material was weighed into fritted tubes. In parallel, 10 equivalents of 9-fluorenylmethyl chloroformate (Fmoc-Cl) was weighed out into a separate glass vial, dissolved in dichloromethane, and mixed with diisopropylethylamine. A quantity of 0.5 mL of this solution was aliquoted into each reaction tube. These tubes were then placed onto an orbital shaker (Vibrax VXR) for 30 min, allowing the Fmoc-Cl coupling reaction to proceed to completion. Excess solvent was removed by pumping on a vacuum block, and the remaining material successively washed with tetrahydrofuran, water, methanol, and dichloromethane (6×1 mL for each solvent). Finally, the samples were dried under nitrogen gas.

Deprotection of the Fmoc-amine groups entailed weighing 10 mg of each dried polymer bead sample into 5 mL volumetric flasks, followed by the addition of 1 mL of a 20% piperidine/*N*,*N*-dimethylformamide solution, and allowing to stand for 30 min. The deprotection product absorbs in the UV region at 301 nm. Therefore each solution was diluted with methanol to make a total of 5 mL, and the absorbance at 301 nm was measured using a UV/Vis spectrometer (Unicam) in conjunction with a reference solution consisting of one part 20% piperidine/*N*,*N*-dimethylformamide to four parts methanol. The Fmoc loading for each sample was calculated using the Beer−Lambert Law.

In the case of Approach B, the samples were sieved into separate particle size ranges after the Fmoc-Cl coupling reaction. In other words, the deprotection of the Fmoc-amines and the determination of Fmoc loading were carried out for each individual particle size range.

The total amount of nitrogen incorporation for the plasma-functionalized polymer spheres (i.e., all types of nitrogen enironment) was quantified by elemental CHN analysis (Exeter Analytical Inc. CE 440 elemental analyzer).

To prepare cross-sections of polystyrene beads for Raman mapping, a thin layer of thermoplastic adhesive (Tempfix, Agar Scientific) was melted onto an aluminum plate (1×1 cm), and polymer beads were sprinkled on top. Cooling to room-temperature immobilized the polymer beads on the adhesive surface. This substrate was then mounted onto a cryogenic microtome (Leica RM 2165), and thin slices were cut off the top of the exposed polymer beads to reveal the cross-sections. Throughout, the temperature of the substrate holder and knife were kept at −20 °C, while the chamber temperature was maintained at −90 °C.

TABLE 1: BET Surface Area and BJH Pore Volume as a Function of Polymer Bead Size

resin	BET surface area (m^2/g)	BJH pore volume (mL/g)
D (20−38)	480 ± 17	0.95 ± 0.06
D (38−53)	478 ± 29	1.00 ± 0.16
D (53−90)	481 ± 50	0.99 ± 0.10
D (90−125)	492 ± 1	0.92 ± 0.12
D (125−180)	493 ± 19	0.92 ± 0.02
D (180−300)	484 ± 6	0.88 ± 0.04

A sample of cross-sectioned, plasma-functionalized polystyrene beads (D (20−38)) was placed in a glass vessel containing 4-cyanobenzoic acid (5 equivalents) and 1,3-diisopropylcarbodiimide (5 equivalents) dissolved in dioxane (1 mL) in order to carry out a coupling reaction between the amine groups and 4-cyanobenzoic acid. The cyano Raman band was used to chemically map the amine functionalities over the cross-sectioned bead.

A Raman microscope system (LABRAM, Jobin Yvon Ltd.) was used to collect intensity profiles, and a two-dimensional chemical map. A Ne−He laser was employed as the excitation source (632.8 nm line, operating at 20 mW). The unattenuated laser beam was focused onto the sample using a microscope objective, and the corresponding Raman signals were collected by the same microscope objective in a backscattering configuration in combination with a cooled CCD detector system. The diffraction gratings (300 grooves grating or 1800 grooves grating) were calibrated against the Si−Si stretching band (521 cm^{-1}) present in the silicon wafer. Individual Raman spectra were obtained using the 300 grooves grating.

Intensity profiles across the bead entailed collecting spectra (750 cm^{-1}−1700 cm^{-1}) along 5 diametric lines over the cross-sectioned beads in 1.0-μm steps. Integration of the ring deformation band[22] (between 980 and 1020 cm^{-1}) produced the intensity-versus-depth profile.

For 2-D chemical mapping, the sample was mounted on a computerized $X-Y$ translational mapping stage and the 1800 grooves grating was selected. The surface was scanned (1830 cm^{-1}−2630 cm^{-1}) using 1.0-μm steps. Integration of the cyano (2210 cm^{-1}−2260 cm^{-1}) band at each pixel provided the overall surface chemical map.

All preparative and analytical experiments were repeated at least in triplicate.

Results and Discussion

Both BET surface area and BJH pore volume values were found to be almost independent of particle size range, within the limits of error, Table 1. Furthermore, the pore size distribution for each of the six different particle size ranges were comparable in most cases, Figure 1. An exception was observed for the three largest particle size ranges, which displayed a somewhat higher number of pores between 500 and 2000 Å. On this basis, it can be assumed that overall, the internal pore architecture of the polymer spheres is similar across all the different particle size ranges employed in this investigation, and hence, the particle size can be taken as being the most influential variable for explaining any observed differences associated with plasmachemical modification.

In the case of Approach A (treatment of individual particle size ranges), it was found that the Fmoc loading (a measure of

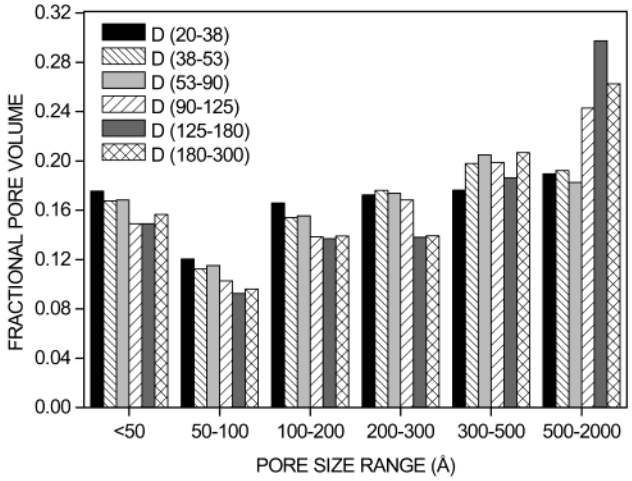

Figure 1. Pore size distribution as a function of particle size. The fractional pore volume is defined as the pore volume of each pore size range divided by the total pore volume for each particle size range.

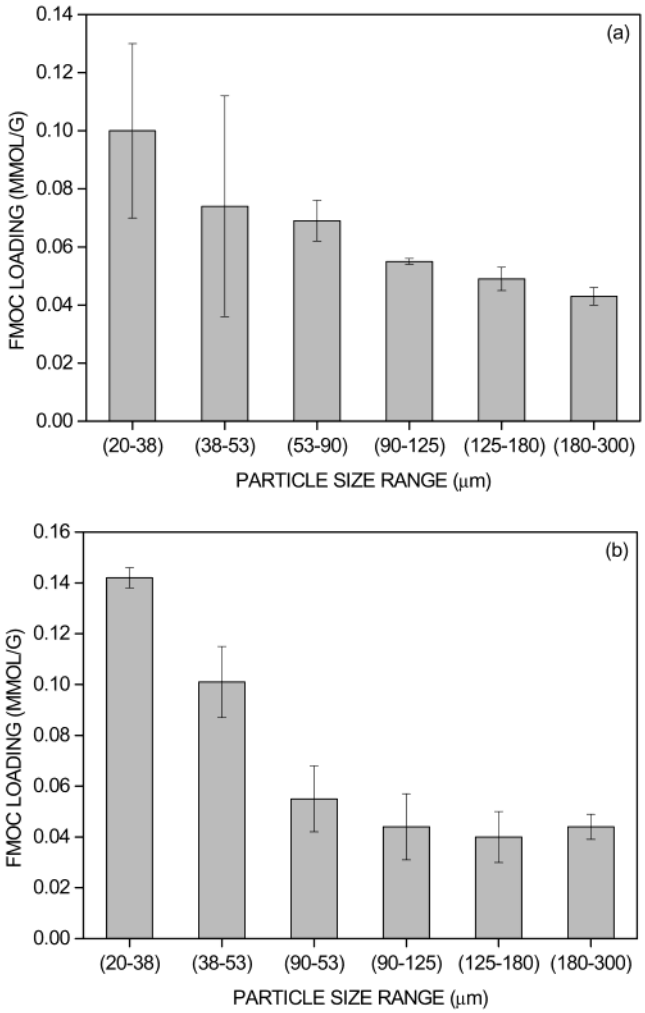

Figure 2. Fmoc loading as a function of particle size range using (a) Approach A, and (b) Approach B.

primary and secondary amines) improved with decreasing particle size, Figure 2a. This would appear to correlate to the fact that the external surface area (i.e., plasma−solid interface) is greater for smaller diameter particles, effectively giving higher plasma accessibility to the internal pore structure. The relatively larger errors observed for the smaller beads (D (20−38) and D (38−53)) can be attributed to the smaller particles being more

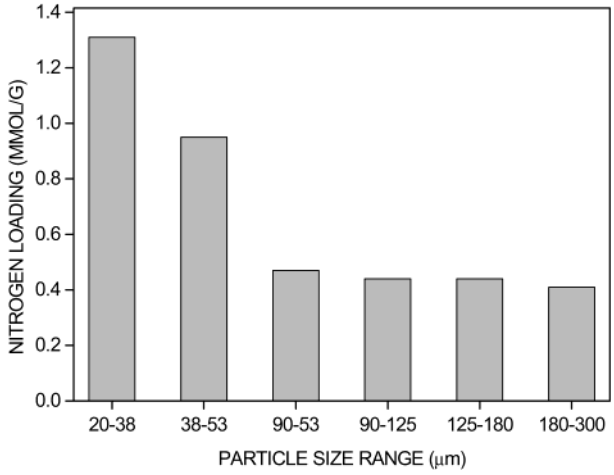

Figure 3. Elemental analysis total nitrogen loading as a function of particle size range using Approach B.

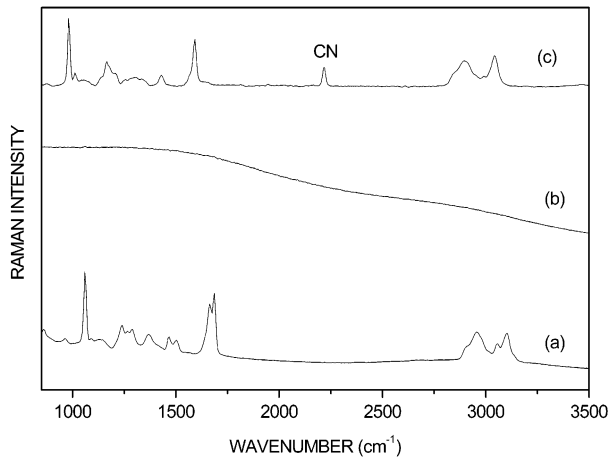

Figure 4. Raman spectra of (a) untreated whole D (20−38) beads; (b) plasma-treated whole D (20−38) beads; and (c) cross-sectioned plasma-treated D (20−38) beads after the coupling reaction with 4-cyanobenzoic acid.

likely to undergo agglomeration during plasma treatment leading to greater fluctuations in the effective plasma−solid interface.

A similar trend was observed in Fmoc loading for Approach B (treatment of mixed particle sizes), with the highest loading correlating to the smallest particles, Figure 2b. However, the smaller particles (D (20−38) and D (38−53)) gave a noticeably higher loading compared to their counterparts in Approach A. This enhancement can be attributed to less agglomeration of smaller particles due to the larger particles in the mixture assisting dispersion while being agitated within the rotating plasma chamber.

The overall nitrogen loading (all types of nitrogen bonding environment) determined by elemental analysis was found to follow the Fmoc trend, despite the values being higher in each case compared to the corresponding Fmoc loading measurements, Figure 3. Therefore not all of the nitrogen-containing functional groups appear to be accessible to the reagents employed during Fmoc analysis. This can be explained in terms of the continuous wave plasma conditions leading to monomer rearrangement and fragmentation to create other types of nitrogen functionality at the surface.[23]

The Raman spectra of polystyrene beads were markedly different before and after allylamine plasma treatment, Figure 4. Disappearance of the characteristic polystyrene ring deformation band (between 980 and 1020 cm^{-1}) is caused by plasma

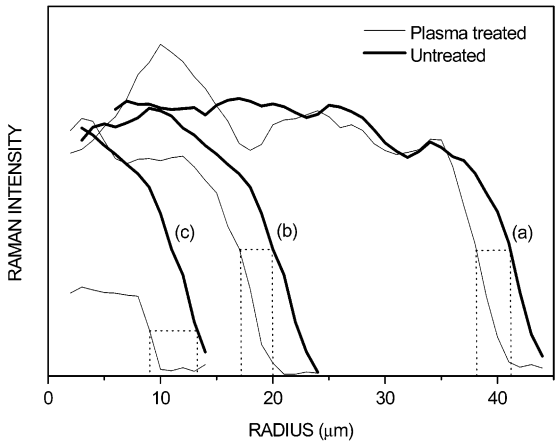

Figure 5. Raman intensity profiles of the integrated polystyrene ring deformation band (between 980 and 1020 cm^{-1}) following cross-sectioning of untreated and plasma-treated beads: (a) D (53−90), (b) D (38−53), and (c) D (20−38). The profiles start from the center and extend outward toward the edge of each bead. The dashed lines highlight the depth of plasma penetration (i.e., untreated versus treated).

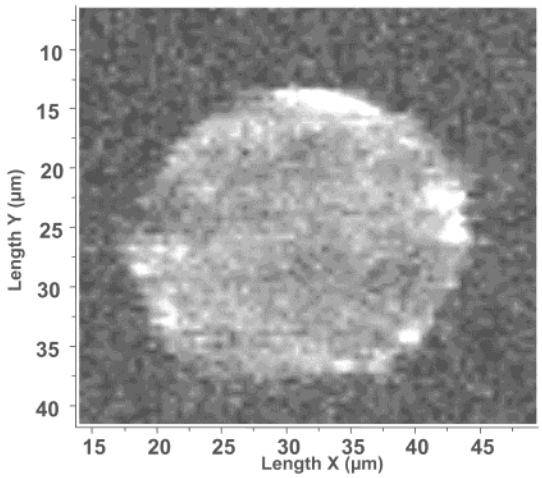

Figure 6. Raman microscopy of allylamine plasmachemical functionalized D (20−38) polystyrene bead following the coupling reaction with 4-cyanobenzoic acid. The bright regions correspond to the integrated cyano band intensity (2210−2260 cm^{-1}).

treatment. A line profile map using the integrated area of this peak as a function of distance across a cross-sectioned bead was used to estimate the depth of plasmachemical modification. Comparison of polystyrene signal profiles for untreated and different size plasma-treated beads shows that plasma penetration is approximately 3 μm for the larger size beads, Figure 5 a and 5b. For the smaller size beads, the plasma treatment is capable of penetrating throughout the particles, since the Raman intensity is notably lower in the center as well, Figure 5c. However, the greatest modification occurs down to a depth of approximately 4 μm.

The distribution of the amine functionalities over cross-sectioned D (20−38) was studied following the coupling reaction with 4-cyanobenzoic acid.[24] The CN band (2232 cm^{-1}) was chosen because it is intense and does not suffer from interference from adjoining peaks, Figure 4c. This reveals that the functional groups are localized near the bead surface, Figure 6. Most of the functionalities are found within a depth of 4 μm from the external surface, while a lower concentration of functional groups is observed toward the bead center. Clearly, the effective amine group density in the near-surface region is in fact much higher than what might appear on the basis of bulk Fmoc analysis. On the basis of this premise, it can be estimated that the effective Fmoc loading is approximately 0.12, 0.16, and 0.39 mmol g^{-1} in the outermost 3−4 μm of 26, 48, and 88 μm diameter polystyrene spheres, respectively. These loadings compare favorably with commercially available conventional bulk functionalized polymer beads. Such high surface densities could potentially be much better suited for loading large biomolecules (e.g., enzymes) onto these materials.[25]

The beauty of the outlined methodology is that other functionalities can also be introduced onto the same base polymer bead, i.e., there is no need for the elaborate wet chemical synthesis of a new material each time. Clearly one might expect there to be a slight variation in the overall functional group density compared to the current study due to the use of a different monomer and plasma processing conditions. However this can be quite easily fine-tuned.

Conclusion

It has been found that the level of plasmachemical amine functionalization of porous polymer beads increases with decreasing particle size. This correlation can be attributed to the effective plasma−solid interfacial area. The chemically accessible amine functionalities are localized near the outer 3−4 μm of each bead.

Acknowledgment. We are grateful to GlaxoSmithKline and EPSRC for Grant GR/M95998.

References and Notes

(1) Rana, S.; Dubuc, J.; Bradley, M.; White, P. *Tetrahedron Lett.* **2000**, *41*, 5135.
(2) Fruchtel, J. S.; Pflugseder, K.; Gstach, H. *Biotechnol. Bioeng.* **2001**, *7*, 94.
(3) Clapham, B.; Sutherland, A. J. *Tetrahedron Lett.* **2000**, *41*, 2253.
(4) Suresh, S.; Skaria, S.; Ponrathnam, S. *Stud. Surf. Sci. Catal.* **1998**, *113*, 915.
(5) Poornanandhan, A. E.; Rajalingam, P.; Radhakrishnan, G. *Polymer* **1993**, *34*, 1485.
(6) Eder, K.; Buchmeiser, M. R.; Bonn, G. K. *J. Chromatogr. A* **1998**, *810*, 43.
(7) Letourneur, D.; Migonney, V.; Muller, D.; Jozefowicz, M. *J. Chromatogr.* **1992**, *589*, 87.
(8) Gaillard, C.; Camps, M.; Proust, J. P.; Hashieh, I. A.; Rolland, P.; Bois, A. *Polymer* **1999**, *41*, 595.
(9) Viklund, C.; Nordstroem, A.; Irgum, K.; Svec, F.; Frechet, J. M. *Macromolecules* **2001**, *34*, 4361.
(10) Denes, F. *Trends Pol. Sci.* **1997**, *5*, 23.
(11) Inagaki, N.; Tasaka, S.; Abe, H. J. *Appl. Polym. Sci.* **1992**, *46*, 595.
(12) Chityala, A.; Van Ooij, W. J. *Surf. Eng.* **2000**, *16*, 299.
(13) Kogoma, M.; Takahashi, R.; Okazaki, S. *Symp. Plasma Sci. Mater.* **1994**, *7th*, 125.
(14) Godfrey, S. P.; Kinmond, E. J.; Badyal, J. P. S.; Little, I. R. *Chem. Mater.* **2001**, *13*, 513.
(15) Koontz, S. L.; Devivar, R. V.; Peltier, W. J.; Pearson, J. E.; Guillory, T. A. *Colloid Polym. Sci.* **1999**, *277*, 557.
(16) Devivar, R. V.; Koontz, S. L.; Peltier, W. J.; Pearson, J. E.; Guillory, T. A.; Fabricant, J. D. *Bioorg. Med. Chem. Lett.* **1999**, *9*, 1239.
(17) Dowding, P. S.; Vincent, B. *Colloids Surf. A* **2000**, *161*, 259.
(18) Barrett, E. P.; Joyner, L. G.; Halenda, P. H. *J. Am. Chem. Soc.* **1951**, *73*, 373.
(19) Sing, K. *Colloids Surf. A* **2001**, *187*, 3.
(20) Brunauer, S.; Emmett, P. H.; Teller, E. *J. Am. Chem. Soc.* **1938**, *60*, 309.
(21) Dörwald, F. Z. *Organic Synthesis on Solid Phase*; Wiley-VCH Verlag: Germany, p 254.
(22) Kress, J.; Rose, A.; Frey, J. G.; Brocklesby, W. S.; Ladlow, M.; Mellor, G. W.; Bradley, M. *Chem. Eur. J.* **2001**, *7*, 3880.
(23) Ganapathy, R.; Wang, X.; Denes, F.; Sarmadi, H. *J. Photopolym. Sci. Technol.* **1995**, *9*, 181.
(24) Nyquist, R. A.; Putzig, C. L.; Leugers, M. A.; McLachlan, R. D.; Thill, B. *Appl. Spectrosc.* **1992**, *46*, 981.
(25) Vágner, J.; Barany, G.; Lam, K. S.; Krchnak, V.; Sepetov, N. F.; Ostrem, J. A.; Strop, P.; Lebl, M. *Proc. Natl. Acad. Sci. U.S.A.* **1996**, *93*, 8194.